

# Tunneling conductance of a mesoscopic ring with spin-orbit coupling and Tomonaga-Luttinger interaction

M. Pletyukhov,<sup>1</sup> V. Gritsev,<sup>2,3</sup> and N. Pauget<sup>1</sup>

<sup>1</sup>*Institut für Theoretische Festkörperphysik, Universität Karlsruhe, D-76128 Karlsruhe, Germany*

<sup>2</sup>*Department of Physics, Harvard University, Cambridge, MA 02138, USA*

<sup>3</sup>*Département de Physique, Université de Fribourg, CH-1700 Fribourg, Switzerland*

Motivated by recent experiments we study the tunneling current through a mesoscopic two-terminal ring with spin-orbit coupling, which is threaded by a magnetic flux. Electron-electron interaction in the ring is described by the Tomonaga-Luttinger model which also allows to account for a capacitive coupling of the ring and the gate electrode. In the regime of weak tunneling, we find how, at temperatures lower than the mean level spacing, the peak positions of the conductance depend on magnetic flux, spin-orbit coupling strength, gate voltage, charging energy and interaction parameters (charge/spin velocity and stiffness). We elucidate the role of the topological modes of a bosonized theory for a finite-size Tomonaga-Luttinger model with periodic boundary conditions, and demonstrate that they are most relevant for the problem in question.

PACS numbers: 73.23.Ad, 71.70.Ej

## I. INTRODUCTION

Mesoscopic rings represent an important tool for experimental and theoretical studies of various phenomena which take place on a submicrometer scale. The ring geometry allows to probe many interesting theoretical predictions. One of the most exciting phenomena is the generation of geometric phases which are manifested in the interference patterns of wavepackets propagating in the ring. Along with the well-known Aharonov-Bohm (AB) effect<sup>1</sup> which takes place for both spinless and spinful particles, the generation of a spin-dependent phase is also possible. This effect, sometimes called the Aharonov-Casher (AC) effect<sup>2</sup>, may occur in the transport of electrons when they are subject to sufficiently strong spin-orbit (SO) coupling. The recent fabrication of HgTe-rings<sup>3</sup> made it possible to directly observe the AC phase. In the earlier experiments with the other compounds<sup>4,5,6</sup> the signatures of this effect have been also detected.

In order to probe the AC phase it is necessary to have a tool for manipulating the strength of spin-orbit coupling. This is provided by the gate-voltage dependence<sup>7</sup> of the Rashba SO coupling<sup>8</sup>, which serves as a basis for a construction of a spin field-effect transistor<sup>9</sup>. Changing the magnetotransport properties of the ring in this way, the experimentalists are now able to study the AC effect<sup>3,4</sup>.

Usually the current through a mesoscopic noninteracting ballistic ring is described theoretically by means of the Landauer-Büttiker scattering matrix theory<sup>10</sup>. Geometric phases arising due to both magnetic flux and SO coupling can be naturally incorporated in this formalism<sup>11,12,13,14,15</sup>. Effects of electron-electron interaction and charging energy are not taken into account in such consideration. However, they might be important, for example, in small quasi-1D rings or in arrays of such rings fabricated in the very recent experiments<sup>4,5,6</sup>.

In the present paper we calculate the linear tunneling conductance of the quasi-1D two-terminal ballistic

ring with Rashba SO coupling threaded by a magnetic flux. The set-up is schematically shown in Fig. 1. The spectrum of electrons in the ring is SO-split into two subbands. We will assume electron densities at which only the lowest radial band is occupied. Electron-electron interaction inside the ring is modeled by the parameters of the Tomonaga-Luttinger liquid (TLL), the leads being noninteracting. Assuming a weak tunneling between the leads and the ring, we compute the leading term of the Kubo conductance perturbatively expanded in a series of tunneling elements. We mostly follow the approach of Ref. 16 where a similar problem for spinless fermions was considered. However, instead of the Matsubara formalism, we apply the Keldysh real-time approach to this quasi-equilibrium problem. We also make use of the bosonization in order to calculate the required TLL correlation functions.

Such a combination of the Keldysh technique and bosonization appears very efficient for a derivation of asymptotic results at temperatures lower than the mean level spacing of the ring's spectrum. In this regime finite-size effects are very important, and the linear conductance is represented by a sequence of peaks when plotted as function of a gate voltage or a magnetic flux<sup>16</sup>. In our paper we focus on the problem how the distribution of the conductance peaks depend on the external parameters (magnetic flux, SO coupling, gate voltage, charging energy) as well as on the parameters of the Tomonaga-Luttinger interaction. The perturbative expansion in tunneling elements is known to break down as soon as the resonance condition is fulfilled. Seeking for the poles of the leading term we are then able to identify the positions of the conductance peaks. Thus, the study of electron transport in the TLL ring provides an effective tool of spectroscopy of its many-body states. Conceptually this is analogous to the study of the tunneling conductance between the two parallel quantum wires<sup>17</sup> which has been realized experimentally<sup>18</sup>. We also note that a description of a shape of a particular peak is a

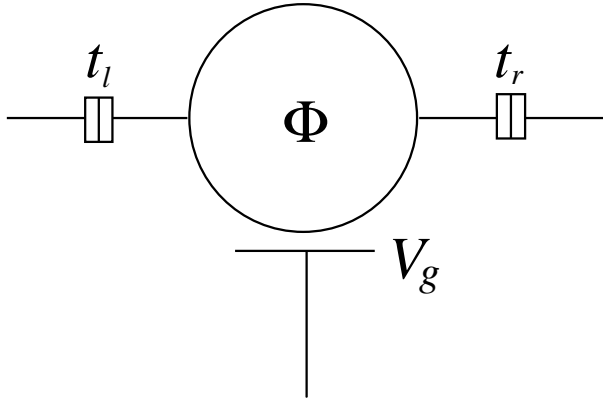


FIG. 1: The ring threaded by a magnetic flux  $\Phi$  is weakly coupled to the leads through the tunneling barriers  $t_l$  and  $t_r$ , and capacitively coupled to the gate electrode ( $V_g$ ).

separate problem which is usually tackled in a somewhat different manner (cf., e.g., Ref. 19), and therefore this issue is not addressed in the present paper.

We underscore the importance of the so-called Klein factors and zero modes (topological excitations) of the bosonized Hamiltonian<sup>20</sup> for our problem. An accurate account of the Klein factors is necessary due to the presence of spin-orbit coupling in the system. The zero-mode sector of TLL decouples from its “continuous” (bosonic) sector, and contains the whole dependence on external parameters<sup>16,21</sup>. The latter appear in the topological sector after imposing boundary conditions. We elaborate the procedure of averaging the conductance over zero modes in presence of spin-orbit coupling, and obtain analytically asymptotic results for the peak positions at temperatures lower than the mean level spacing. We also revisit the case of spinless fermions reproducing the result of Ref. 16 and discussing it in further detail.

It is worthwhile to note that the relevance of the topological modes for a description of mesoscopic phenomena in the TLL rings has been already appreciated in various contexts, including the studies of persistent<sup>22</sup> and Josephson currents<sup>21</sup>, and the study of AB phase in the chiral Luttinger liquids<sup>23</sup>. The structure of the topological sector in presence of SO coupling has been recently discussed as well in application to persistent<sup>24,25</sup> and Josephson<sup>26</sup> currents.

The paper is organized as follows. In Sec. II we briefly outline the construction of the spectrum of the ring with SO coupling. In Sec. III we summarize the results emerging from an application of the Landauer-Büttiker formalism to this system. They will be further used as a reference in the noninteracting limit. In Sec. IV we present a derivation of the Kubo formula in the real-time approach. Briefly reviewing the bosonization formalism in Sec. V, we derive an expression for the dc conductance to be averaged over zero modes. The procedure of averaging is performed in Sec. VI. We discuss the interplay of the externally tuned and interaction parameters in the

distribution of the conductance peaks, especially focusing on the modification of the Coulomb blockade due to SO coupling.

## II. MESOSCOPIC RINGS WITH RASHBA COUPLING: DISPERSION RELATIONS

The two-dimensional electron gas with Rashba spin-orbit coupling is described by the Hamiltonian

$$H = \frac{1}{2m^*}(p_x^2 + p_y^2) + \alpha_R(\sigma_x p_y - \sigma_y p_x) + V(r), \quad (1)$$

where  $r = \sqrt{x^2 + y^2}$ . The magnetic field  $\mathbf{B}$  is introduced in the kinetic momentum  $\mathbf{p} \rightarrow \mathbf{p} + \frac{e}{c}\mathbf{A}$  via the gauge potential  $\mathbf{A} = \frac{B}{2}(-y, x, 0)$ . The radial potential  $V(r)$  confining an electron to the ring geometry can be modeled, for example, either by singular isotropic harmonic oscillator or by concentric hard walls<sup>25</sup>. For these or any other types of the radial confinement the resulting quasi-one-dimensional spectrum  $\epsilon_{n\sigma}(k)$  is labeled by the radial band index  $n = 0, 1, \dots$ , by the angular momentum  $\hbar k = \dots, -\hbar, 0, \hbar, \dots$ , and by the subband index (chirality)  $\sigma = \pm$ . From now on we will put  $\hbar = 1$ .

If the effective ring’s width is much smaller than the ring’s radius, we can neglect the hybridization between the radial bands. We also assume electron densities at which only the lowest radial band ( $n = 0$ ) is occupied. Thus, we effectively consider the strictly one-dimensional spectrum (see Fig. 2) which has a parabolic shape and is SO-split into two subbands<sup>25</sup>

$$\epsilon_\sigma(k) \equiv \epsilon_{0\sigma}(k) = \frac{2\pi^2}{m^* L^2}(k - k_\Phi - \sigma k_R)^2. \quad (2)$$

Here  $L$  is the ring’s perimeter,  $k_\Phi = \Phi/\Phi_0$  is a number of flux quanta  $\Phi_0$  threading the ring, and the parameter

$$k_R = \sqrt{\frac{1}{4} + \left(\frac{\alpha_R m^* L}{2\pi}\right)^2} - \frac{1}{2} \quad (3)$$

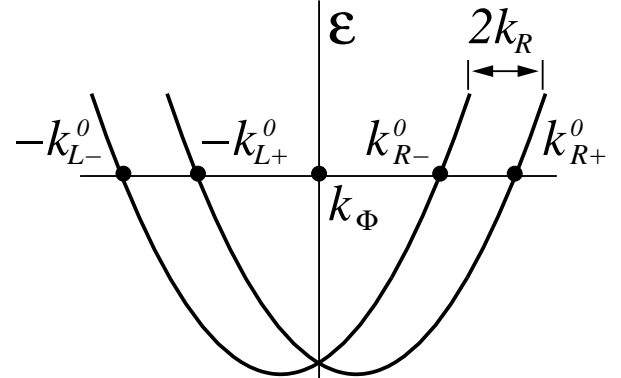


FIG. 2: The lowest radial band of the quasi-1D mesoscopic ring SO-split into two subbands.

depends on the Rashba coupling  $\alpha_R$ .

Linearizing the spectrum (2) near the Fermi energy, we obtain the four branches

$$\varepsilon_{\eta\sigma}(k) = \omega_0(k - k_{\eta\sigma}^0) \equiv \omega_0(k - \eta k_F - k_\Phi - \sigma k_R), \quad (4)$$

specified by  $\eta = \pm$  (or  $\eta = R, L$ ) and  $\sigma = \pm$ . The Fermi angular velocity  $\omega_0 = \left(\frac{2\pi}{L}\right)^2 \frac{k_F}{m^*}$  defines the level spacing of the spectrum (4), and  $k_F$  is the Fermi angular momentum in absence of magnetic field and SO coupling.

### III. CONDUCTANCE OF THE MESOSCOPIC RING: NONINTERACTING ELECTRONS

Let us consider the conductance of the ring attached to the semi-infinite leads (Fig. 1). For non-interacting

electrons it can be easily found in the framework of the scattering matrix theory<sup>10</sup>.

$$G(k_F, k_\Phi) = \frac{e^2}{2\pi} \frac{16\epsilon_l\epsilon_r \sin^2 k_F \pi \cos^2 k_\Phi \pi}{[-2\alpha_l\alpha_r + (1 + \gamma_l\gamma_r) \cos 2\pi k_F - 2\beta_l\beta_r \cos 2\pi k_\Phi]^2 + (1 - \gamma_l\gamma_r)^2 \sin^2 2\pi k_F}, \quad (5)$$

where  $\epsilon_{l/r}$ ,  $\gamma_{l/r} = -\sqrt{1 - 2\epsilon_{l/r}}$ ,  $\alpha_{l/r} = -\frac{1}{2}(1 + \gamma_{l/r})$ , and  $\beta_{l/r} = \frac{1}{2}(1 - \gamma_{l/r})$  are the phenomenological parameters describing scattering in a T-shaped (left  $l$  or right  $r$ ) junction. The number of flux quanta is given by  $k_\Phi = \frac{1}{2}(k_R^0 - k_L^0)$ , while the quantity  $k_F = \frac{1}{2}(k_R^0 + k_L^0)$  corresponds to the Fermi momentum at zero flux. It can be replaced by  $k_F \rightarrow N_0 + \frac{\Delta\mu}{\omega_0}$ , where  $\Delta\mu$  is a difference between the chemical potential of the leads and the Fermi energy of the ring, and the integer  $N_0$  is related to the number  $2N_0 + 1$  of electrons in the ring at  $\Delta\mu = 0$ . Since the expression (5) is periodic in  $k_F$ , the integer part of  $k_F$  can be discarded. Thus, the conductance (5) actually depends on the fractional part of  $\frac{\Delta\mu}{\omega_0}$ . For the future references we introduce the parameter  $k_\mu = \frac{\Delta\mu}{\omega_0} - \frac{1}{2}$ .

In the low tunneling limit  $\epsilon_{l/r} \ll 1$  the conductance (5) approximately equals

$$G \approx \frac{e^2}{2\pi} \frac{4\epsilon_l\epsilon_r \sin^2 k_F \pi \cos^2 k_\Phi \pi}{(\cos 2\pi k_F - \cos 2\pi k_\Phi)^2 + \frac{1}{4}(\epsilon_l + \epsilon_r)^2 \sin^2 2\pi k_F}. \quad (6)$$

As a function  $k_\mu$  and  $k_\Phi$ , it represents a sequence of Breit-Wigner resonances. The conductance peaks occur when the resonance condition  $\cos 2\pi k_F = \cos 2\pi k_\Phi$  is fulfilled, i.e. at the values of parameters

$$k_F + k_\Phi = n_R, \quad k_F - k_\Phi = n_L, \quad (7)$$

where  $n_R$  and  $n_L$  are arbitrary integers.

It has been demonstrated in Ref. 12 that for electrons with nonzero SO coupling and negligible Zeeman splitting the conductance of the mesoscopic ring is given by the sum of the two contributions:  $G(k_F, k_\Phi + k_R)$  and

It is instructive to consider first the case of spinless fermions with the two linearization points  $k_{R/L}^0$ . One finds that in the zero-temperature limit and for the angle  $\pi$  between the leads the dc conductance reads<sup>10</sup>

$G(k_F, k_\Phi - k_R)$ . In other words, the net effect of the SO coupling for noninteracting electrons is the generation of the different effective flux values for the different channels. Therefore, the pattern of the conductance maxima at  $k_R \neq 0$  is determined by the resonance conditions

$$k_F + (k_\Phi \pm k_R) = n_{R\pm}, \quad k_F - (k_\Phi \pm k_R) = n_{L\pm}, \quad (8)$$

where  $n_{R\pm}$  and  $n_{L\pm}$  are arbitrary integers. Recalling that effectively  $k_\mu = k_F - \frac{1}{2}$ , we show in Fig. 3 how the arrangement of the conductance peaks is modified by SO coupling.

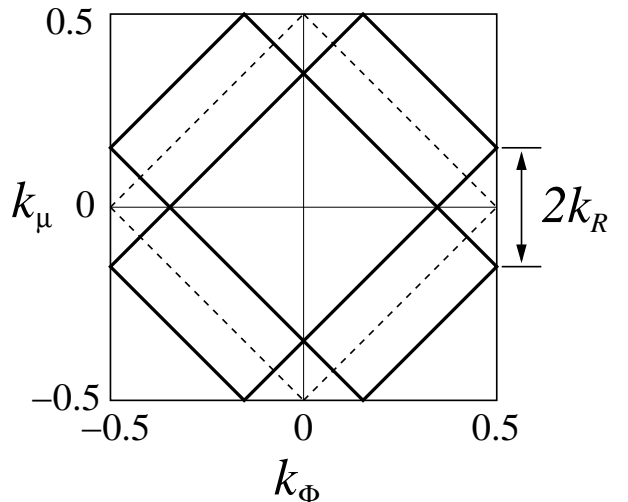


FIG. 3: Splitting of the conductance peaks (solid lines) due to SO coupling. The dashed lines correspond to  $k_R = 0$ .

#### IV. KUBO FORMULA

In order to take into account effects of electron-electron interaction on the distribution of conductance peaks, we discuss in this section the Kubo formula for the linear conductance. Although this expression is very standard, we re-derive it using the Keldysh formalism. In doing this, we pursue the two objectives. First, we would like to have a better control of the approximations used (similar to those made in Ref. 16). Second, we would like to deduce an expression for the conductance in the real-time representation. Its advantage for the ring geometry will be discussed in the next section where the calculation of time-dependent finite-size TLL correlation functions is concerned.

In the second-quantized formulation the mesoscopic ring attached to the leads is described by the Hamiltonian

$$H = H_l + H_r + H_c + H_T. \quad (9)$$

The left/right lead is described by a Fermi-liquid Hamiltonian  $H_{l/r} = \int dx c_{l/r}^\dagger(x) \left( \frac{p^2}{2m^*} - \mu \right) c_{l/r}(x)$ , and the tunneling term is  $H_T = \sum_{l,r} (t_{l/r} c_{l/r}^\dagger(x_{l/r}) \psi(x_{l/r}) + \text{h.c.})$ . Here  $c_{l/r}$  and  $\psi$  are the field operators in the leads and in the ring, respectively.

The Hamiltonian of the central part (ring)  $H_c[\psi^\dagger, \psi]$  can have any interaction term in addition to the ki-

netic term. In our consideration we will model electron-electron interaction in the ring by the Tomonaga-Luttinger liquid which includes only forward scattering processes (“density-density” type interaction). In the framework of this model it is also possible to take into account the charging effects. They originate from a capacitive coupling of the ring to the gate electrode, and are described by the Hamiltonian  $E_c(N_{ring} - \frac{1}{e} C_g V_g)^2$ , with the charging energy  $E_c = e^2/2C_g$ . Here  $C_g$  is the gate capacitance, and  $\hat{N}_{ring}$  is the ring’s number operator.

Linear response of the system to an applied time-dependent bias voltage is described by the Kubo formula for the ac conductance<sup>27</sup>

$$G(\Omega) = -\frac{1}{\Omega} \int_{-\infty}^t dt' e^{-i\Omega(t'-t)} \langle [\hat{I}_l(t), \hat{I}_r(t')] \rangle, \quad (10)$$

where  $\hat{I}_{l/r}(t) = ie \left( t_{l/r} \hat{c}_{l/r}^\dagger(x_{l/r}, t) \hat{\psi}(x_{l/r}, t) - \text{h.c.} \right)$  is a current operator in the left/right junction written in the Heisenberg representation.

In the low tunneling limit the expression (10) can be expanded in a series of  $H_T$ . We make use of the real-time Keldysh diagrammatic technique, and for  $t > t'$  we replace  $\langle [\hat{I}_l(t), \hat{I}_r(t')] \rangle$  by

$$\langle T_t \hat{I}_l(t) \hat{I}_r(t') \rangle - \langle \tilde{T}_t \hat{I}_l(t) \hat{I}_r(t') \rangle \equiv 2i \text{Im} \langle T_t \hat{I}_l(t) \hat{I}_r(t') \rangle. \quad (11)$$

When expressed on the Keldysh contour, it reads

$$\langle T_t \hat{I}_l(t), \hat{I}_r(t') \rangle = \langle \tilde{T}_t e^{i \int_{-\infty}^t H_T(t'') dt''} I_l(t) T_t e^{-i \int_{-\infty}^t H_T(t'') dt''} \tilde{T}_t e^{i \int_{-\infty}^{t'} H_T(t'') dt''} I_r(t') T_t e^{-i \int_{-\infty}^{t'} H_T(t'') dt''} \rangle, \quad (12)$$

where the operators without hats refer to the interaction ( $H_T$ ) representation.

Expanding (11) to the second order in  $H_T$ , we obtain

$$\begin{aligned} & \int_{-\infty}^t dt_1 \int_{-\infty}^{t'} dt'_1 \langle [[I_l(t), H_T(t_1)], [H_T(t'_1), I_r(t')]] \rangle \\ & - \int_{-\infty}^t dt_1 \int_{-\infty}^{t_1} dt_2 \langle [[[I_l(t), H_T(t_1)], H_T(t_2)], I_r(t')] \rangle \\ & - \int_{-\infty}^{t'} dt'_1 \int_{-\infty}^{t'_1} dt'_2 \langle [I_l(t), [H_T(t'_2), [H_T(t'_1), I_r(t')]]] \rangle. \end{aligned}$$

The next step is to perform averaging over the leads’ states. While doing this, we meet the following combinations: (a)  $(G_l^R - G_l^A)(G_r^R - G_r^A)$ ; (b)  $G_l^K(G_r^R - G_r^A)$ ; (c)  $(G_l^R - G_l^A)G_r^K$ ; (d)  $G_l^K G_r^K$ . Here  $G_{l/r}^{R,A}$  and  $G_{l/r}^K$  are the momentum-averaged retarded, advanced and Keldysh

functions of the leads in the real-time representation

$$\begin{aligned} (G^R - G^A)_{l/r}(t) &= -i \langle \{c_{l/r}(t), c_{l/r}^\dagger(0)\} \rangle = -2\pi i \delta(t) \frac{\nu_{l/r}}{V_{l/r}}, \\ G_{l/r}^K(t) &= -i \langle [c_{l/r}(t), c_{l/r}^\dagger(0)] \rangle = -\frac{2\pi}{\beta \sinh(\pi t/\beta)} \frac{\nu_{l/r}}{V_{l/r}}, \end{aligned}$$

and  $\nu_{l/r}$  is the density of states in the left/right lead at the Fermi level.

One can straightforwardly prove that the combinations (a) and (b) vanish identically. The combination (c) gives the following contribution to the conductance

$$\begin{aligned} G^{(c)}(\Omega) &= e^2 \Gamma_l \Gamma_r L^2 \int_{-\infty}^0 \int_{-\infty}^0 dt_1 dt_2 \frac{e^{-i\Omega t_1} (1 - e^{-i\Omega t_2})}{2i\Omega \beta \sinh[\pi t_2/\beta]} \\ & \times \text{Re} \langle \{ [[\psi_l(0), \psi_l^\dagger(0)], \psi_r(t_1)], \psi_r^\dagger(t_1 + t_2) \} \rangle, \end{aligned} \quad (13)$$

where  $\Gamma_{l/r} = 2\pi\nu_{l/r}|t_{l/r}|^2/(V_{l/r}L)$ , and  $V_{l/r}$  is a volume of the left/right lead.

From (13) we derive an expression for the dc conductance ( $\Omega = 0$ ) at zero temperature

$$G^{(c)} = \frac{e^2}{2\pi} \Gamma_l \Gamma_r L^2 \int_{-\infty}^0 \int_{-\infty}^0 dt_1 dt_2 \times \text{Re}\langle \{[[\psi_l(0), \psi_l^\dagger(0)], \psi_r(t_1)], \psi_r^\dagger(t_1 + t_2)\} \rangle \quad (14)$$

Using the operator identities

$$\{[C, A], B\} + \{[C, B], A\} = [C, \{A, B\}], \quad (15)$$

$$\{C, \{A, B\}\} - \{A, \{C, B\}\} = [[C, A], B], \quad (16)$$

we rewrite (14)

$$G^{(c)} = \frac{e^2}{4\pi} \Gamma_l \Gamma_r L^2 \int_{-\infty}^0 \int_{-\infty}^0 dt_1 dt_2 \times \left\{ \text{Re}\langle \{[[\psi_l(0), \psi_l^\dagger(0)], \psi_r(t_1)], \psi_r^\dagger(t_2)\} \rangle + \text{Re}\langle [[\psi_l(0), \psi_l^\dagger(0)], \{\psi_r(t_1), \psi_r^\dagger(t_2)\}] \rangle \right\}, \quad (17)$$

and further express

$$\begin{aligned} & \langle \{[[\psi_l(0), \psi_l^\dagger(0)], \psi_r(t_1)], \psi_r^\dagger(t_2)\} \rangle \\ &= \langle \{\{\psi_l(0), \psi_r^\dagger(t_2)\}, \{\psi_r(t_1), \psi_l^\dagger(0)\}\} \rangle \\ &+ \langle [[\psi_r^\dagger(t_2), \{\psi_l^\dagger(0), \psi_r(t_1)\}], \psi_l(0)\rangle \\ &- \langle \{\{\psi_l^\dagger(0), \{\psi_l(0), \psi_r(t_1)\}\}, \psi_r^\dagger(t_2)\} \rangle. \end{aligned} \quad (18)$$

It is obvious that in the noninteracting limit the only term  $\langle \{\{\psi_l(0), \psi_r^\dagger(t_2)\}, \{\psi_r(t_1), \psi_l^\dagger(0)\}\} \rangle$  survives, since the other terms vanish due to the fermionic commutation relations. We approximate the dc conductance in the interacting case by this dominant contribution

$$G \approx \frac{e^2}{4\pi} \Gamma_l \Gamma_r L^2 \int_{-\infty}^0 \int_{-\infty}^0 dt_1 dt_2 \times \text{Re}\langle \{\{\psi_l(0), \psi_r^\dagger(t_2)\}, \{\psi_r(t_1), \psi_l^\dagger(0)\}\} \rangle. \quad (19)$$

Splitting the four-particle correlator, one can recover the formula  $G \approx (e^2/2\pi) \Gamma_l \Gamma_r L^2 |G^R(\omega = 0, x_l - x_r)|^2$  from Ref. 16, where  $G^R(\omega = 0, x_l - x_r)$  is a zero-frequency retarded Green's function for interacting electrons in the ring. This approximation physically means that one scattering event is completed before another takes place. In general, the TLL correlation functions of any order can be calculated within the bosonization approach, and this approximation can be relaxed.

The combination (d) with  $G_l^K G_r^K$  also gives a finite contribution to the conductance, which, however, vanishes in the noninteracting limit as well. Therefore, we will neglect it on the same ground as we have just neglected the subdominant terms in (17) and (18).

## V. BOSONIZATION

### A. Spinless case

In order to compute the four-particle correlator (19), we will make use of the bosonization technique<sup>20</sup>.

Let us consider for simplicity the spinless case. We introduce the short-hand notations for the fermionic fields  $\psi_l \equiv \psi(x_l)$  and  $\psi_r \equiv \psi(x_r)$ , where  $x_l$  and  $x_r$  are the angle coordinates of the left and right junctions. In the following we assume that  $x_l = 0$  and  $x_r = \pi$ .

In the bosonization the fields  $\psi_{l/r}$  are represented as a sum of the right ( $\eta = +$ , or  $R$ ) and the left ( $\eta = -$ , or  $L$ ) moving components

$$\psi_{l/r} = \psi_{l/r,R} + \psi_{l/r,L} = F_{l/r,R} \psi_{l/r,R}^b + F_{l/r,L} \psi_{l/r,L}^b, \quad (20)$$

and each of  $\psi_{l/r,\eta}$  consists of a topological part  $F_{l/r,\eta}$  and a bosonic part  $\psi_{l/r,\eta}^b$  commuting with each other:  $[F, \psi^b] = 0$ .

The bosonic part is given by

$$\begin{aligned} \psi_\eta^b(x) &= \frac{1}{\sqrt{L\tilde{\alpha}}} e^{-i\sqrt{2\pi}\phi_\eta(x)}, \\ \phi_\eta(x) &= i \sum_{k=1}^{\infty} \frac{e^{-\frac{1}{2}\tilde{\alpha}k}}{\sqrt{2\pi k}} \left( e^{i\eta kx} b_{\eta k} - e^{-i\eta kx} b_{\eta k}^\dagger \right), \end{aligned} \quad (21)$$

where  $\tilde{\alpha} = \frac{2\pi\alpha}{L}$  is a small dimensionless cut-off parameter, and the operators  $b_{\eta k}$ ,  $b_{\eta k}^\dagger$  satisfy the bosonic commutation relation:  $[b_{\eta k}, b_{\eta' k'}^\dagger] = \delta_{\eta\eta'} \delta_{kk'}$ .

The topological part is important for the finite-size TLL with periodic boundary conditions. It includes Klein factors  $F_\eta$ , zero-mode operators  $N_\eta$ , and the linearization points  $k_\eta^0$  (see Fig. 2 assuming  $k_R = 0$ ):

$$F_{l/r,\eta} = F_\eta e^{i\eta(N_\eta - k_\eta^0)x_{l/r}}. \quad (22)$$

The zero-mode operators  $N_\eta = N_\eta^\dagger$  take integer values, and the following relations are satisfied<sup>20</sup>

$$[F_\eta, N_{\eta'}] = F_\eta \delta_{\eta\eta'}, \quad (23)$$

$$\{F_\eta, F_{\eta'}^\dagger\} = 2\delta_{\eta\eta'}, \quad (24)$$

$$\{F_\eta, F_{\eta'}\} = \{F_\eta^\dagger, F_{\eta'}^\dagger\} = 0 \quad \text{for } \eta \neq \eta'. \quad (25)$$

The bosonized TLL Hamiltonian  $H_{TLL} \equiv H_c = H_b + H_0$  consists of a “continuous” (bosonic)  $H_b$  and a topological  $H_0$  parts which are decoupled from each other. Therefore, the factorization of  $\psi_{l/r,\eta}$  into  $F_{l/r,\eta}$  and  $\psi_{l/r,\eta}^b$  takes place at any time instant

$$\psi_{l/r}(t) = F_{l/r,R}(t) \psi_{l/r,R}^b(t) + F_{l/r,L}(t) \psi_{l/r,L}^b(t), \quad (26)$$

where the time evolutions of  $\psi_{l/r,\eta}^b(t)$  and  $F_{l/r,\eta}(t)$  are governed by  $H_b$  and  $H_0$ , respectively. By the same reason the statistical averaging in both bosonic and topological sectors are independent of each other.

The bosonic part of the TLL Hamiltonian is given by

$$H_b = \frac{2\pi v}{L} \sum_{a=1,2} \sum_{k=1}^{\infty} k d_{ak}^\dagger d_{ak}, \quad (27)$$

where  $v$  is the so-called charge velocity (the renormalization of the Fermi velocity  $v_0 \equiv \frac{L\omega_0}{2\pi}$ ). The operators  $d_{ak}$ ,

$d_{ak}^\dagger$  ( $a = 1, 2$ ) are obtained from  $b_{\eta k}, b_{\eta k}^\dagger$  by the canonical transformation (A1). The latter depends on the interaction parameter  $\gamma = \frac{1}{2}(\frac{1}{K} + K)$ , where  $K$  is the so-called charge stiffness. For repulsive interactions  $K < 1$ , while in the non-interacting limit  $K = \gamma = 1$  and  $v = v_0$ .

The topological part of the TLL Hamiltonian is

$$H_0 = \sum_{\eta} \left( a_0 \tilde{N}_{\eta}^2 + a_1 \tilde{N}_{\eta} \tilde{N}_{-\eta} \right), \quad (28)$$

where  $a_{0,1} = \frac{\omega_0}{4}(\tilde{\nu} \pm \lambda)$  and

$$\tilde{\nu} = \nu + \frac{4E_c}{\omega_0}, \quad \nu = \frac{v}{Kv_0}, \quad \lambda = \frac{vK}{v_0}. \quad (29)$$

The topological numbers  $\tilde{N}_{\eta} = N_{\eta} - k_{\eta}$  are shifted by  $k_{\eta} = k_{\eta}^0 + \delta k_{\mu}$ , where

$$\delta k_{\mu} = \frac{4E_c(\frac{1}{e}C_g V_g - 2N_0) + 2\Delta\mu - \omega_0}{2\tilde{\nu}\omega_0} \quad (30)$$

re-defines the linearization points  $k_{\eta}^0$  in order to include the dependence on  $\Delta\mu$  and the gate voltage  $V_g$ . In the basis  $N = N_R + N_L, J = N_R - N_L$ , the Hamiltonian  $H_0$  acquires the diagonal form

$$H_0 = \frac{\omega_0}{4}[\tilde{\nu}\tilde{N}^2 + \lambda\tilde{J}^2], \quad (31)$$

where  $\tilde{N} = N - 2k_{\mu}$ ,  $\tilde{J} = J - 2k_{\Phi}$ , and  $k_{\mu} = N_0 + \delta k_{\mu}$ . One can observe that the whole dependence on  $\Delta\mu, V_g$  and  $\Phi$  is included in the topological sector.

Using the commutation relations (23) we find the time evolution of the Klein factors

$$F_{\eta}(t) = e^{iH_0 t} F_{\eta} e^{-iH_0 t} = e^{-itP_{\eta} + ita_0}, \quad (32)$$

where

$$P_{\eta} = 2a_0 \tilde{N}_{\eta} + 2a_1 \tilde{N}_{-\eta} = \frac{\omega_0}{2}[\tilde{\nu}\tilde{N} \pm \lambda\tilde{J}]. \quad (33)$$

The details of the time evolution of the bosonic fields are presented in Appendix A. In fact, they are not very important for our purpose. We will only exploit the fact that the average of the bosonic fields

$$g^b(t; \gamma) = \langle \psi_{lR}^b(t) \psi_{rR}^{b\dagger}(0) \rangle \equiv \langle \psi_{lL}^b(t) \psi_{rL}^{b\dagger}(0) \rangle \quad (34)$$

is a periodic function of time which can be expanded in a Fourier series

$$g^b(t; \gamma) = \sum_{p=0}^{\infty} g_p(\gamma) e^{-ip\omega t} \quad (35)$$

with the frequency  $\omega = \frac{2\pi v}{L}$  and the real-valued coefficients  $g_p(\gamma)$ . Note that the summation in (35) is performed only over non-negative integers.

The real-time periodicity of  $g^b(t; \gamma)$  is inherited from the spatial periodic boundary conditions. The occurrence of the Fourier series (35) allows us to perform all time

integrals explicitly. The analysis of the remaining series is a much simpler task.

Let us make yet another approximation in the spirit of Ref. 16. In particular, we split the four-particle bosonic correlator in (19) neglecting the anomalous averages (e.g.,  $\langle \psi^b \psi^b \rangle$ ), the left-right mixing (e.g.,  $\langle \psi_L^b \psi_R^{b\dagger} \rangle$ ) and the vertex corrections (averages of operators at the same spatial point, e.g.,  $\langle \psi_r^b \psi_r^{b\dagger} \rangle$ ) in the *bosonic* (continuous) sector. At the same time, we do not split the topological part of the four-particle correlator (unlike it has been done in Ref. 16), and perform a single averaging of the whole over zero modes.

Implementing this procedure, we obtain

$$\begin{aligned} \langle \psi_l(0) \psi_r^\dagger(t_2) \psi_r(t_1) \psi_l^\dagger(0) \rangle &\approx g^{b*}(t_2) g^b(t_1) \\ &\times \sum_{\eta_1, \eta_2} \left\langle F_{l, \eta_2}(0) F_{r, \eta_2}^\dagger(t_2) F_{r, \eta_1}(t_1) F_{l, \eta_1}^\dagger(0) \right\rangle_{z.m.} \end{aligned} \quad (36)$$

where  $\langle \dots \rangle_{z.m.}$  implies averaging over zero modes to be discussed later. Collecting all contributions, we find

$$\begin{aligned} G &\approx \frac{e^2}{2\pi} \Gamma_l \Gamma_r L^2 \sum_{p_1, p_2=0}^{\infty} g_{p_1}(\gamma) g_{p_2}(\gamma) \int_{-\infty}^0 \int_{-\infty}^0 dt_1 dt_2 \\ &\times \sum_{\eta} \text{Re} \left\langle \left( e^{it_1(\omega p_1 + a_0 + P_{\eta})} - e^{-it_1(\omega p_1 + a_0 - P_{\eta})} \right) \right. \\ &\quad \times \left. \left( e^{-it_2(\omega p_2 + a_0 + P_{\eta})} - e^{it_2(\omega p_2 + a_0 - P_{\eta})} \right) \right\rangle_{z.m.} \\ &+ e^{i(N_{\eta} + N_{-\eta})\pi} \left( e^{i\eta t_1(\omega p_1 + a_0 + P_{\eta})} - e^{-i\eta t_1(\omega p_1 + a_0 - P_{\eta})} \right) \\ &\quad \times \left. \left( e^{-i\eta t_2(\omega p_2 + a_0 + P_{-\eta})} - e^{i\eta t_2(\omega p_2 + a_0 - P_{-\eta})} \right) \right\rangle_{z.m.}. \end{aligned} \quad (37)$$

Introducing

$$A_{\eta}^{\pm} = \sum_{p=0}^{\infty} \frac{g_p(\gamma)}{\omega p + a_0 \pm P_{\eta}} \quad (38)$$

and  $A_{\eta} = A_{\eta}^+ + A_{\eta}^-$ , we can cast Eq. (37) into the form

$$\begin{aligned} G &\approx \frac{e^2}{2\pi} \Gamma_l \Gamma_r L^2 \left\langle A_R^2 + A_L^2 \right. \\ &\quad \left. + 2A_R A_L \cos(\tilde{N}_R + \tilde{N}_L + 2\delta k_{\mu})\pi \right\rangle_{z.m.}. \end{aligned} \quad (39)$$

We need to establish an efficient procedure of averaging over zero modes. But first we observe the modification of the conductance caused by the presence of spin degrees of freedom and by spin-orbit coupling.

## B. Spinful case

Performing a similar bosonization procedure in the spinful case, we obtain the following expression for the dc conductance

$$\begin{aligned} G &\approx \frac{e^2}{2\pi} \Gamma_l \Gamma_r L^2 \sum_{\sigma} \left\langle A_{R\sigma}^2 + A_{L\sigma}^2 \right. \\ &\quad \left. + 2A_{R\sigma} A_{L\sigma} \cos(\tilde{N}_{R\sigma} + \tilde{N}_{L\sigma} + 2\delta k_{\mu})\pi \right\rangle_{z.m.}. \end{aligned} \quad (40)$$

The zero-mode operators  $N_{\eta\sigma}$  with integer eigenvalues are shifted to  $\tilde{N}_{\eta\sigma} = N_{\eta\sigma} - k_{\eta\sigma}$  by  $k_{\eta\sigma} = k_{\eta\sigma}^0 + \delta k_\mu$ , where

$$\delta k_\mu = \frac{4E_c(\frac{1}{e}C_gV_g - 4N_0) + 2\Delta\mu - \omega_0}{2\tilde{\nu}_c\omega_0}. \quad (41)$$

The integer  $N_0 = \frac{1}{4}\sum_{\eta,\sigma} k_{\eta\sigma}^0$  is related to the number  $4N_0 + 2$  of electrons in the ring when the parameters

$$k_\Phi = \frac{1}{4}\sum_\sigma (k_{R\sigma} - k_{L\sigma}), \quad (42)$$

$$k_{B,R} = \frac{1}{4}\sum_\sigma \sigma(k_{R\sigma} \pm k_{L\sigma}), \quad (43)$$

equal zero. The parameter  $k_B$  vanishes in the absence of Zeeman interaction. The parameter

$$k_\mu = \frac{1}{4}\sum_{\eta,\sigma} k_{\eta\sigma} = N_0 + \delta k_\mu \quad (44)$$

contains the dependence on  $\Delta\mu$  and  $V_g$ .

Like in the spinless case, it is convenient to introduce

$$\tilde{\nu}_c = \nu_c + \frac{8E_c}{\omega_0}, \quad \nu_{c,s} = \frac{v_{c,s}}{K_{c,s}v_0}, \quad \lambda_{c,s} = \frac{v_{c,s}K_{c,s}}{v_0}, \quad (45)$$

and  $\omega_{c,s} = \frac{2\pi v_{c,s}}{L}$ ,  $\gamma_{c,s} = \frac{1}{2}(\frac{1}{K_{c,s}} + K_{c,s})$ , which are expressed through the charge and spin velocities  $v_c \neq v_s$ , the charge and spin stiffnesses  $K_c \neq K_s$ , and the charging energy  $E_c$ .

In Eq. (40) the rates  $\Gamma_l$  and  $\Gamma_r$  remain the same as in the spinless case, since we assume that the density of states in the leads is spin-independent, and equals  $\nu_{l/r}$  for each spin component. The spin dependence appears in the functions  $A_{\eta\sigma} = A_{\eta\sigma}^+ + A_{\eta\sigma}^-$ ,

$$A_{\eta\sigma}^\pm = \sum_{p_c,p_s=0}^{\infty} \frac{g_{p_c}(\frac{1}{2}\gamma_c)g_{p_s}(\frac{1}{2}\gamma_s)}{\omega_c p_c + \omega_s p_s + \bar{a}_0 \pm P_{\eta\sigma}}, \quad (46)$$

$$P_{\eta\sigma} = 2\bar{a}_0\tilde{N}_{\eta\sigma} + 2\bar{a}_1\tilde{N}_{-\eta,\sigma} + 2\bar{a}_2\tilde{N}_{\eta,-\sigma} + 2\bar{a}_3\tilde{N}_{-\eta,-\sigma}. \quad (47)$$

The coefficients  $\bar{a}_{0,1} = \frac{\omega_0}{8}(\tilde{\nu}_c \pm \lambda_c + \nu_s \pm \lambda_s)$  and  $\bar{a}_{2,3} = \frac{\omega_0}{8}(\tilde{\nu}_c \pm \lambda_c - \nu_s \mp \lambda_s)$  are the components of the quadratic form of the zero-mode Hamiltonian

$$H_0 = \sum_{\eta,\sigma} \left( \bar{a}_0\tilde{N}_{\eta\sigma}^2 + \bar{a}_1\tilde{N}_{\eta\sigma}\tilde{N}_{-\eta,\sigma} + \bar{a}_2\tilde{N}_{\eta\sigma}\tilde{N}_{\eta,-\sigma} + \bar{a}_3\tilde{N}_{\eta\sigma}\tilde{N}_{-\eta,-\sigma} \right). \quad (48)$$

In the basis

$$N_{c,s} = (N_{R+} + N_{L+}) + \sigma(N_{R-} + N_{L-}), \quad (49)$$

$$J_{c,s} = (N_{R+} - N_{L+}) + \sigma(N_{R-} - N_{L-}), \quad (50)$$

the Hamiltonian (48) becomes diagonal

$$H_0 = \frac{\omega_0}{8} \left[ \tilde{\nu}_c\tilde{N}_c^2 + \lambda_c\tilde{J}_c^2 + \nu_s\tilde{N}_s^2 + \lambda_s\tilde{J}_s^2 \right], \quad (51)$$

and

$$P_{\eta\sigma} = \frac{\omega_0}{4} \left[ (\tilde{\nu}_c\tilde{N}_c + \eta\lambda_c\tilde{J}_c) + \sigma(\nu_s\tilde{N}_s + \eta\lambda_s\tilde{J}_s) \right], \quad (52)$$

where  $\tilde{N}_{c,s} = N_{c,s} - 4k_{\mu,B}$  and  $\tilde{J}_{c,s} = J_{c,s} - 4k_{\Phi,R}$ .

In the Eq. (40) the two components  $\sigma = \pm$  seem to be independent of each other. However, this is not the case, and they are, in fact, entangled due to the non-trivial procedure of averaging over zero modes.

## VI. AVERAGING OVER ZERO MODES

### A. Spinless case

The typical expression to be averaged over zero modes before the time integration has the form [cf. Eq. (37)]

$$\langle e^{ib_1\tilde{N}+ib_2\tilde{J}} \rangle_{z.m.} = \frac{\text{Tr}(e^{ib_1\tilde{N}+ib_2\tilde{J}} e^{-\beta H_0})}{\text{Tr}(e^{-\beta H_0})}, \quad (53)$$

where  $b_{1,2}$  depend linearly on the time arguments  $t_{1,2}$ . The trace operation is understood as a summation over all possible integer values of  $N_L$  and  $N_R$ . In the basis  $(N, J)$  we have to sum over either both even  $(2m, 2n)$  or both odd  $(2m+1, 2n+1)$  eigenvalues. Thus,

$$\begin{aligned} \text{Tr}(e^{-\beta H_0}) &= \sum_{m,n=-\infty}^{\infty} e^{-\beta\omega_0[\tilde{\nu}(m-k_\mu)^2 + \lambda(n-k_\Phi)^2]} \\ &+ \sum_{m,n=-\infty}^{\infty} e^{-\beta\omega_0[\tilde{\nu}(m+\frac{1}{2}-k_\mu)^2 + \lambda(n+\frac{1}{2}-k_\Phi)^2]} \\ &= \frac{\pi}{\beta\omega_0\sqrt{\tilde{\nu}\lambda}} \left[ \theta_3\left(\pi k_\mu, e^{-\frac{\pi^2}{\beta\omega_0\tilde{\nu}}}\right) \theta_3\left(\pi k_\Phi, e^{-\frac{\pi^2}{\beta\omega_0\lambda}}\right) \right. \\ &\quad \left. + \theta_4\left(\pi k_\mu, e^{-\frac{\pi^2}{\beta\omega_0\tilde{\nu}}}\right) \theta_4\left(\pi k_\Phi, e^{-\frac{\pi^2}{\beta\omega_0\lambda}}\right) \right], \end{aligned} \quad (54)$$

where  $\theta_{3,4}$  are the Jacobian theta functions. Some properties of these functions are reviewed in Appendix B.

The numerator in (53) can be equivalently rewritten in the form

$$\text{Tr}\left(e^{ib_1\tilde{N}+ib_2\tilde{J}} e^{-\beta H_0}\right) = \text{Tr}\left(e^{-\beta H'_0}\right) \cdot e^{-\frac{1}{\beta\omega_0}\left(\frac{b_1^2}{\tilde{\nu}} + \frac{b_2^2}{\lambda}\right)}, \quad (55)$$

where  $H'_0$  is obtained from  $H_0$  by replacing

$$k_\mu \rightarrow k'_\mu = k_\mu + \frac{ib_1}{\beta\omega_0\tilde{\nu}}, \quad (56)$$

$$k_\Phi \rightarrow k'_\Phi = k_\Phi + \frac{ib_2}{\beta\omega_0\lambda}. \quad (57)$$

At low temperatures  $\beta^{-1} \ll \omega_0, E_c$ , the last exponential factor in (55) can be discarded. Using (B5) we derive the following expression

$$\begin{aligned} \langle e^{ib_1\tilde{N}+ib_2\tilde{J}} \rangle_{z.m.} &\approx p_1(k_\mu, k_\Phi) e^{2ib_1 f(k_\mu) + 2ib_2 f(k_\Phi)} \\ &\quad + p_2(k_\mu, k_\Phi) e^{2ib_1 f(k_\mu+1/2) + 2ib_2 f(k_\Phi+1/2)}. \end{aligned} \quad (58)$$

The ‘‘saw-tooth’’ function

$$f(x) = \sum_{n=1}^{\infty} \frac{(-1)^n}{\pi n} \sin 2\pi n x \quad (59)$$

has the period 1 and equals  $f(x) = -x$  for  $x \in (-\frac{1}{2}, \frac{1}{2})$ , and  $f(\pm\frac{1}{2}) = 0$ . The functions  $p_{1,2}(k_\mu, k_\Phi)$  are determined by

$$\begin{aligned} p_1(k_\mu, k_\Phi) &= \frac{1}{1 + \frac{\theta_4(\pi k_\mu, e^{-\pi^2/\beta\omega_0\tilde{\nu}})\theta_4(\pi k_\Phi, e^{-\pi^2/\beta\omega_0\lambda})}{\theta_3(\pi k_\mu, e^{-\pi^2/\beta\omega_0\tilde{\nu}})\theta_3(\pi k_\Phi, e^{-\pi^2/\beta\omega_0\lambda})}} \\ &\approx \frac{1}{1 + e^{\beta\omega_0[\tilde{\nu}g_2(k_\mu) + \lambda g_2(k_\Phi)]}}, \end{aligned} \quad (60)$$

and  $p_2(k_\mu, k_\Phi) = p_1(k_\mu + \frac{1}{2}, k_\Phi + \frac{1}{2})$ . One can observe that  $p_1 + p_2 = 1$ . The function  $g_2(x)$  is introduced in (B9).

Let us consider the limit of zero temperature, or  $\beta \rightarrow \infty$ . The expression (58) becomes exact in this limit. Since  $b_1$  and  $b_2$  are linear in time, we can perform easily all time integrations. Thus, the averaging over zero modes effectively results in replacing  $\tilde{N} \rightarrow 2f(k_\mu + \frac{1}{2}\delta_{\mu 1(2)})$  and  $\tilde{J} \rightarrow 2f(k_\Phi + \frac{1}{2}\delta_{\Phi 1(2)})$ , where  $\delta_{\mu 1} = \delta_{\Phi 1} = 0$  and  $\delta_{\mu 2} = \delta_{\Phi 2} = 1$ , which assumes further summation over the different topological realizations (1 and 2) of the ground state with the weight factors  $p_1$  and  $p_2$ . For  $\beta^{-1} \ll \omega_0$  the latter approximately equal

$$p_1(k_\mu, k_\Phi) = \Theta(-\tilde{\nu}g_2(k_\mu) - \lambda g_2(k_\Phi)), \quad (61)$$

$$p_2(k_\mu, k_\Phi) = \Theta(\tilde{\nu}g_2(k_\mu) + \lambda g_2(k_\Phi)), \quad (62)$$

and play the role of projectors which divide the elementary cell  $(k_\Phi, k_\mu) \in [-\frac{1}{2}, \frac{1}{2}] \times [-\frac{1}{2}, \frac{1}{2}]$  into two areas (topological sectors).

Let us analyze such partition of the elementary cell, and consider the (upper right) quadrant defined by  $0 < k_\mu < \frac{1}{2}$  and  $0 < k_\Phi < \frac{1}{2}$ . The function  $g_2(x) = x - 1/4$  for  $0 < x < 1/2$ , and therefore the border between the areas of  $p_1$  and  $p_2$  is given by the equation

$$\tilde{\nu}k_\mu + \lambda k_\Phi = \frac{\tilde{\nu} + \lambda}{4}. \quad (63)$$

For repulsive interactions and, moreover, in the presence of  $E_c \neq 0$  the relation  $\tilde{\nu}/\lambda > 1$  is fulfilled.

We can establish the borders between the topological sectors  $p_1$  and  $p_2$  in the other quadrants by mirroring (63) with respect to  $k_\mu$ -axis,  $k_\Phi$ -axis or both. Thus, we obtain that the area of the projector  $p_1$  is the inner part of the elementary cell bounded by the hexagon (see Fig. 4). Respectively, the outer part is the area of  $p_2$ .

Let us now analyze the conductance in the upper right quadrant. In the inner part  $p_1$  only the zero harmonic ( $p = 0$ ) of  $A_R^+$  becomes divergent near the border line (63). In the outer part  $p_2$  the zero harmonic ( $p = 0$ ) of  $A_R^-$  is divergent near the border line (63). From the both sides of the latter the conductance behaves like

$$G \propto \frac{1}{[\tilde{\nu}k_\mu + \lambda k_\Phi - \frac{\tilde{\nu}+\lambda}{4}]^2}. \quad (64)$$

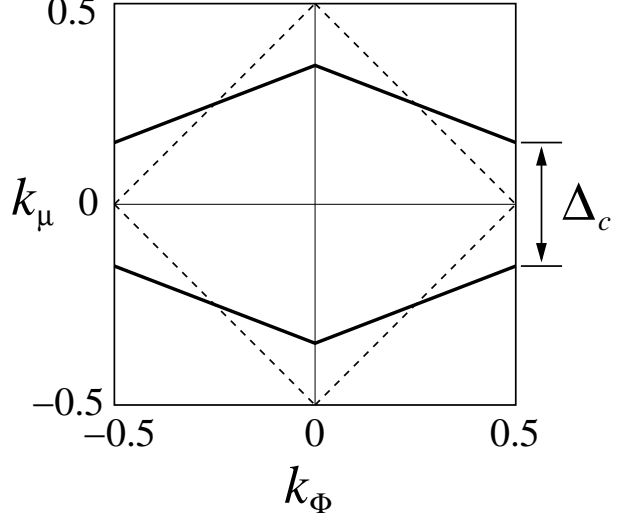


FIG. 4: Shift of the conductance peaks (solid lines) due to the charging energy. The dashed lines correspond to the non-interacting case ( $\Delta_c = 0$ ).

This is an expected result as well as the fact that the pole of the conductance (condition for the resonant tunneling of an electron) matches with a transition  $p_1 \rightarrow p_2$  from one topological sector to another.

In order to identify the positions of the conductance peaks, it appears sufficient to consider just the zero harmonics  $p = 0$  of the functions  $A_\eta^\pm$ , because the higher ones ( $p \geq 1$ ) do not have any poles at all.

It is instructive to derive the conductance in the non-interacting limit  $\tilde{\nu} = \lambda = 1$ . Using the identity

$$\frac{\pi}{\sin \pi x} = \sum_{p=-\infty}^{\infty} \frac{(-1)^p}{p + x}, \quad (65)$$

one can show that

$$G = \frac{e^2}{2\pi} \frac{\Gamma_l \Gamma_r}{\omega_0^2} \left[ \frac{\pi}{\sin(\frac{\Delta\mu}{\omega_0} + k_\Phi)\pi} + \frac{\pi}{\sin(\frac{\Delta\mu}{\omega_0} - k_\Phi)\pi} \right]^2. \quad (66)$$

This result can be recovered in the scattering matrix approach, if the width of the Breit-Wigner resonance in (6) is neglected. The expression (66) suggests that the resonant condition can be satisfied at any  $k_\mu$  by tuning the magnetic flux  $k_\Phi$ .

As it was discussed in Ref. 16, the main qualitative feature imposed by electron-electron interaction and/or charging energy is the opening of a window at the certain values of  $k_\mu$  inside which the resonant condition is never met. This situation is shown in Fig. 4, and the corresponding gap value equals  $\Delta_c = \frac{1}{2}(1 - \frac{\lambda}{\tilde{\nu}})$ .

## B. Spinful case

In order to implement an averaging similar to (53) in the spinful cases, it is necessary to calculate first the par-

partition function  $\text{Tr}(e^{-\beta H_0})$ . The trace operation is now understood as a summation over all integer values of  $N_{R+}$ ,  $N_{L+}$ ,  $N_{R-}$ ,  $N_{L-}$ . However, in this basis the Hamiltonian (48) is not diagonal, and we have to use the basis (49),(50) instead. The summation rules for the latter have been formulated, for instance, in Refs. 21,24,25. Applying them, one can find that the partition function is proportional to

$$\sum_{i=1}^{16} \left[ \theta_3 \left( \pi k_{\mu i}, e^{-\frac{\pi^2}{2\beta\omega_0\nu_c}} \right) \theta_3 \left( \pi k_{\Phi i}, e^{-\frac{\pi^2}{2\beta\omega_0\lambda_c}} \right) \right. \\ \left. \times \theta_3 \left( \pi k_{Bi}, e^{-\frac{\pi^2}{2\beta\omega_0\nu_s}} \right) \theta_3 \left( \pi k_{Ri}, e^{-\frac{\pi^2}{2\beta\omega_0\lambda_s}} \right) \right], \quad (67)$$

where  $k_{Xi} = k_X + \frac{1}{4}\delta_{Xi}$  ( $X = \mu, \Phi, B, R$ ), and the summation is performed over 16 topological sectors. The latter are specified by  $\delta_{Xi}$  given in the table

$i$	1	2	3	4	5	6	7	8	9	10	11	12	13	14	15	16
$\delta_{\mu i}$	0	2	2	0	2	2	0	0	1	3	3	1	3	3	1	1
$\delta_{\Phi i}$	0	2	2	0	0	0	2	2	1	3	3	1	1	1	3	3
$\delta_{Bi}$	0	2	0	2	2	0	2	0	1	3	1	3	3	1	3	1
$\delta_{Ri}$	0	2	0	2	0	2	0	2	1	3	1	3	1	3	1	3

One can define 16 functions ( $i = 1, \dots, 16$ )

$$p_i(k_X) = p_1(k_{Xi}), \quad (68)$$

where  $p_1(k_X)$  equals to

$$\frac{1}{1 + \sum_{j=2}^{16} \frac{\theta_3(\pi k_{\mu j})}{\theta_3(\pi k_\mu)} \frac{\theta_3(\pi k_{\Phi j})}{\theta_3(\pi k_\Phi)} \frac{\theta_3(\pi k_{B j})}{\theta_3(\pi k_B)} \frac{\theta_3(\pi k_{R j})}{\theta_3(\pi k_R)}} \\ \approx \frac{1}{1 + \sum_{j=2}^{16} e^{2\beta\omega_0 B_j(k_X)}}, \quad (69)$$

and the functions  $B_j(k_X)$  are introduced in Appendix B.

The functions (68) satisfy the identity

$$\sum_{i=1}^{16} p_i(k_X) = 1. \quad (70)$$

At low temperatures  $\beta^{-1} \ll \omega_0$  we have an approximate relation

$$p_1(k_X) = \prod_{j=2}^{16} \Theta(-B_j(k_X)), \quad (71)$$

and the functions  $p_i(k_X)$  become the projectors which divide the elementary cell  $k_X \in [-\frac{1}{2}, \frac{1}{2}] \times \dots \times [-\frac{1}{2}, \frac{1}{2}]$  in the four-dimensional parameter space into 16 topological sectors.

We can now formulate the rule which prescribes how to evaluate the average over zero modes in (40): it is necessary to replace

$$\tilde{N}_c \rightarrow 4f(k_{\mu i}), \quad \tilde{J}_c \rightarrow 4f(k_{\Phi i}), \quad (72)$$

$$\tilde{N}_s \rightarrow 4f(k_{Bi}), \quad \tilde{J}_s \rightarrow 4f(k_{Ri}), \quad (73)$$

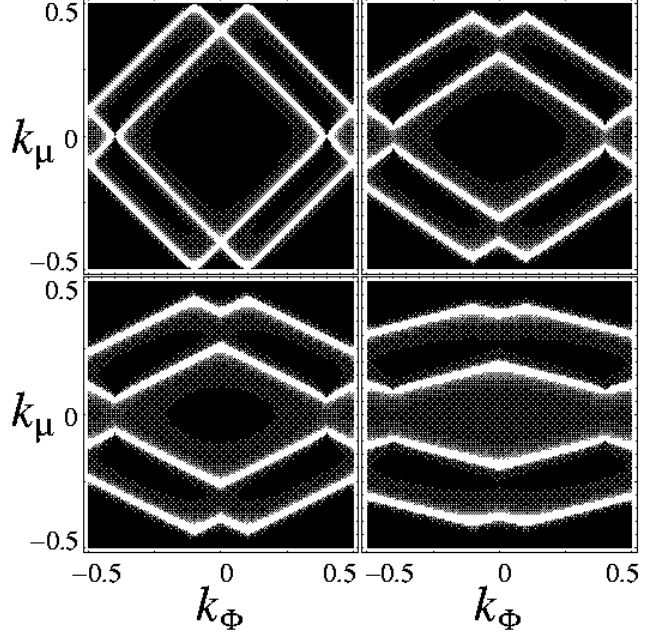


FIG. 5: Conductance peaks for  $k_R = 0.1$  and different values of the charging energy  $8E_c/\omega_0 = 0.0$  (upper left), 0.5 (upper right), 1.0 (bottom left), 3.0 (bottom right). The TLL parameters are  $\nu_{c,s} = \lambda_{c,s} = 1$ .

and to sum over  $i = 1, \dots, 16$  topological realization of the ground state with the weight functions  $p_i(k_X)$ .

Once this procedure is implemented, it becomes sufficient to consider just the zero harmonics ( $p_c = p_s = 0$ ) of the functions  $A_{\eta\sigma}^\pm$  (46) for establishing the positions of the conductance maxima. In this respect there exists the full analogy with the spinless case, and we refer to the corresponding discussion in the previous subsection.

In the framework of the developed formalism it is possible to study the influence of the TLL interaction on the distribution of the conductance peaks in presence of magnetic flux and SO coupling. The charging effects are also naturally incorporated, and the charging energy  $E_c$  plays a role similar to that of the TLL parameter  $\nu_c$ . They are both combined into  $\tilde{\nu}_c$  (see Eq. (45)), and therefore the effects produced by each of them are analogous. Let us then fix  $\nu_c = 1$  and vary  $E_c$ . In Fig. 5 we show the elementary cells of the conductance contour-plot in the  $(k_\Phi, k_\mu)$ -plane for  $k_R = 0.1$  and different values of the charging energy. The TLL parameters are  $\nu_{c,s} = \lambda_{c,s} = 1$ . One can see how the separate effects of SO coupling and charging energy (shown in Fig. 3 and Fig. 4, respectively) merge together.

In experiments the usual tuning parameters are  $\Phi$  and  $V_g$ . The parameter  $V_g$  appears in the theoretical model through both  $k_R$  and  $k_\mu$ . The Rashba coupling constant depends on an applied gate voltage<sup>7</sup>, which is modeled by  $\alpha_R = \alpha_R^0 - \frac{\pi}{m^* L} \kappa v_g$ , where  $v_g = \frac{eV_g}{\omega_0}$ , and  $\kappa > 0$  is a dimensionless coefficient. The degeneracy point in gate voltage at which the Rashba coupling  $\alpha_R$  vanishes

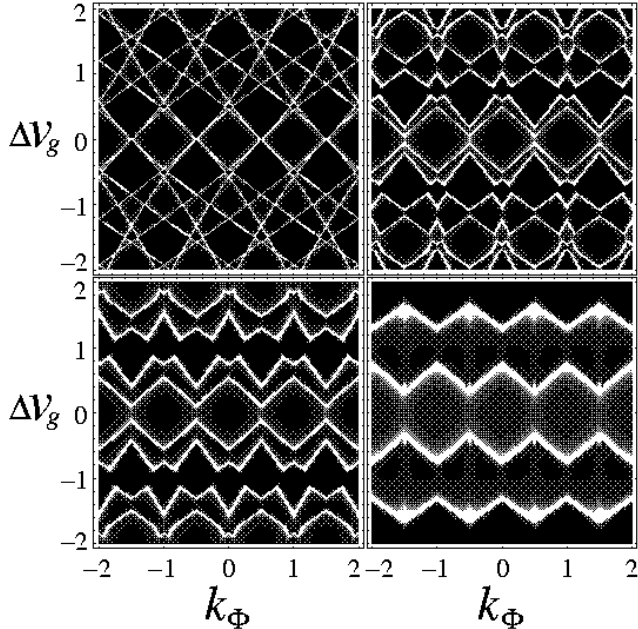


FIG. 6: Conductance peaks for  $\kappa = 1$  and different values of the charging energy  $8E_c/\omega_0 = 0.0$  (upper left), 0.5 (upper right), 1.0 (bottom left), 3.0 (bottom right).

is defined by  $v_g^0 \equiv v_g(\alpha_R = 0) = \frac{m^* L \alpha_R^0}{\kappa \pi}$ . Introducing the departure from the degeneracy point  $\Delta v_g = v_g - v_g^0$ , we then express

$$k_R(\Delta v_g) = \frac{1}{2} \left( \sqrt{1 + \kappa^2(\Delta v_g)^2} - 1 \right) \quad (74)$$

and

$$k_\mu(\Delta v_g) = \frac{\Delta v_g + v'}{1 + 8E_c/\omega_0}. \quad (75)$$

Here  $v' = v_g^0 + \frac{\Delta \mu}{\omega_0} + N_0 - \frac{1}{2}$  determines the shift of the whole pattern, we may put at will  $v' = 0$ .

In Fig. 6 we demonstrate the influence of the charging effects in  $(k_\Phi, \Delta v_g)$ -plane. The values of  $E_c$  and  $\nu_{c,s}$ ,  $\lambda_{c,s}$  are the same as in Fig. 5. We observe that upon enhancement of the charging energy the gap opens near  $\Delta v_g = 0$ . Due to the presence of the gate-dependent SO coupling, the pattern of conductance maxima is more complicated than that discussed in Ref. 16.

## VII. DISCUSSION AND CONCLUSION

In this work we have studied the tunneling conductance of a mesoscopic one-dimensional ring attached to two Fermi reservoirs. The interaction inside the ring is described by the Tomonaga-Luttinger liquid. The bosonization approach which is usually adopted for the study of such model allows to include the flux and gate-voltage dependence as well as the influence of SO coupling. It

is remarkable that all these externally tuned parameters appear in the topological sector of the bosonized theory. Therefore, the accurate treatment of zero modes is required in order to describe the mesoscopic phenomena at low temperatures  $\beta^{-1} \ll \omega_0$ .

Using the Keldysh formalism we have performed the calculation of a linear conductance in the limit of weak tunneling between the leads and the ring. The real-time approach allows to obtain asymptotic results for the distribution of the conductance peaks in the low temperature limit. Although the perturbative expansion of the conductance in the tunneling strength is not very well suited for a description of a shape of conductance peaks, it is nevertheless quite efficient for establishing their positions. The topological origin of the peaks' distribution alludes to its robustness upon small modifications of the model.

We have studied the patterns of the conductance maxima at nonzero spin-orbit coupling as a function of magnetic flux and gate voltage. The Tomonaga-Luttinger interaction and the charging energy have been seen to contribute in analogous way. In rings of the reduced size the account of charging effects might appear more experimentally motivated, and therefore we concentrated on their study. In particular, we have made a theoretical prediction for the distribution of the conductance peaks in presence of both the charging energy and the spin-orbit coupling. We observed an interesting interplay between the both effects. The SO coupling lifts the degeneracy of the conduction peaks, and the charging energy opens a gap centered at the remaining points of the degeneracy in question. The value of this gap is proportional to the charging energy. When the latter becomes very large, the Rashba effect is less pronounced. The pattern of the conductance peaks then approaches the form of hexagonal honeycombs which is typical to spinless fermions.

In conclusion, we have described the interplay between Coulomb blockade and Aharonov-Bohm and Aharonov-Casher effects for the different values of the charging energy, magnetic flux and spin-orbit coupling, as it is manifested in the contour-plots of the tunneling conductance.

## Acknowledgments

We would like to thank Dmitry Bagrets, Thierry Champel and Gerd Schön for fruitful discussions. M.P. was supported by the DFG Center for Functional Nanostructures at the University of Karlsruhe. V.G. was supported by the Swiss National Science Foundation.

## APPENDIX A: CORRELATION FUNCTIONS OF THE TOMONAGA-LUTTINGER MODEL

Let us consider for simplicity the spinless case. The canonical transformation which solves the two-channel

TLL model is

$$\begin{pmatrix} d_{1k} \\ d_{2k}^\dagger \end{pmatrix} = \begin{pmatrix} u_+ & u_- \\ u_- & u_+ \end{pmatrix} \begin{pmatrix} b_{Rk} \\ b_{Lk}^\dagger \end{pmatrix}, \quad (\text{A1})$$

where  $u_\pm = \sqrt{(\gamma \pm 1)/2}$ .

The explicit form of the time evolution of the bosonized fields reads

$$\psi_\eta^b(x, t) = \frac{1}{\sqrt{L\tilde{\alpha}}} e^{-i\sqrt{2\pi}\phi_\eta(x, t)}, \quad (\text{A2})$$

$$\begin{aligned} \phi_\eta(x, t) &= i \sum_{k=1}^{\infty} \frac{e^{-\frac{1}{2}\tilde{\alpha}k}}{\sqrt{2\pi k}} \\ &\times [u_\eta D_{1k}(x - \omega t) - u_{-\eta} D_{2k}(x + \omega t)], \end{aligned} \quad (\text{A3})$$

where

$$D_{1k} = e^{ikx} d_{1k} - e^{-ikx} d_{1k}^\dagger, \quad (\text{A4})$$

$$D_{2k} = e^{ikx} d_{2k}^\dagger - e^{-ikx} d_{2k}. \quad (\text{A5})$$

Let us consider the correlation function

$$\begin{aligned} \langle \psi_\eta^b(x, t) \psi_\eta^{b\dagger}(x, t) \rangle &= e^{-\pi(\langle (\phi_\eta(x, t) - \phi_\eta)^2 \rangle + \pi[\phi_\eta(x, t), \phi_\eta])} \\ &= e^{-u_+^2(\pi\mathcal{D}(\eta x - \omega t) - i\chi(\eta x - \omega t))} \\ &\times e^{-u_-^2(\pi\mathcal{D}(\eta x + \omega t) + i\chi(\eta x + \omega t))}, \end{aligned} \quad (\text{A6})$$

where

$$\mathcal{D}(x) = \frac{1}{\pi} \sum_{k=1}^{\infty} \frac{1 - \cos kx}{k} \left( \frac{2}{e^{\beta\omega k} - 1} + e^{-\tilde{\alpha}k} \right), \quad (\text{A7})$$

$$\chi(x) = \sum_{k=1}^{\infty} \frac{\sin kx}{k} e^{-\tilde{\alpha}k} = \frac{1}{2i} \ln \frac{1 - e^{-ix - \tilde{\alpha}}}{1 - e^{ix - \tilde{\alpha}}} \quad (\text{A8})$$

are the periodic functions of  $x$ . Obviously, the function (A6) is also periodic in real time, and therefore it can be expanded in the Fourier series with the frequency  $\omega$ .

In the zero-temperature limit  $\beta \rightarrow \infty$  the temperature-dependent part of  $\mathcal{D}(x)$  can be discarded, and we obtain

$$\mathcal{D}(x) = -\frac{1}{2\pi} \ln \frac{(1 - e^{-\tilde{\alpha}})^2}{(1 - e^{-ix - \tilde{\alpha}})(1 - e^{ix - \tilde{\alpha}})}. \quad (\text{A9})$$

Hence, the correlation function (A6) equals to

$$\left( \frac{1 - e^{-\tilde{\alpha}}}{1 - e^{i(\eta x - \omega t + i\tilde{\alpha})}} \right)^{u_+^2} \left( \frac{1 - e^{-\tilde{\alpha}}}{1 - e^{-i(\eta x + \omega t - i\tilde{\alpha})}} \right)^{u_-^2}. \quad (\text{A10})$$

For  $x = \pi$  we have

$$\langle \psi_\eta^b(\pi, t) \psi_\eta^{b\dagger}(\pi, t) \rangle = \frac{1}{L\tilde{\alpha}} \left( \frac{1 - e^{-\tilde{\alpha}}}{1 + e^{-i\omega t - \tilde{\alpha}}} \right)^\gamma. \quad (\text{A11})$$

Its Fourier expansion (35) is equivalent to the Taylor expansion of the analytic function  $(1 + z)^{-\gamma}$  for  $|z| < 1$ .

Therefore the expansion (35) contains only non-negative Fourier harmonics ( $p \geq 0$ ) with the coefficients

$$\begin{aligned} g_p(\gamma) &= \frac{(-1)^p \Gamma(p + \gamma)}{\Gamma(\gamma) \Gamma(p + 1)} \frac{(1 - e^{-\tilde{\alpha}})^\gamma}{L\tilde{\alpha}} e^{-p\tilde{\alpha}} \\ &\approx \frac{(-1)^p \Gamma(p + \gamma)}{\Gamma(\gamma) \Gamma(p + 1)} \frac{\tilde{\alpha}^{\gamma-1}}{L}. \end{aligned} \quad (\text{A12})$$

Computation of a correlation function in the spinful case is analogous. A new feature arising in this case is the double time-periodicity of correlation functions with frequencies  $\omega_c$  and  $\omega_s$ , which are in general incommensurate.

## APPENDIX B: JACOBIAN THETA FUNCTIONS

The Jacobian function  $\theta_3$  is defined by

$$\theta_3(z, q) = 1 + 2 \sum_{n=1}^{\infty} q^{n^2} \cos 2nz, \quad (\text{B1})$$

and the Jacobian function  $\theta_4$  can be expressed as

$$\theta_4(z, q) = \theta_3 \left( z + \frac{\pi}{2}, q \right). \quad (\text{B2})$$

Both functions are periodic under the shift  $z \rightarrow z + \pi$ .

Making Poisson summation, one can prove that

$$\sum_{k=-\infty}^{\infty} e^{-a(k+z)^2} = \sqrt{\frac{\pi}{a}} \theta_3 \left( \pi z, e^{-\pi^2/a} \right). \quad (\text{B3})$$

Using the expression for the ratio of two  $\theta_3$ -functions

$$\ln \frac{\theta_3(z_1 + z_2, q)}{\theta_3(z_1 - z_2, q)} = 4 \sum_{n=1}^{\infty} \frac{(-1)^n}{n} \frac{q^n}{1 - q^{2n}} \sin 2nz_1 \sin 2nz_2, \quad (\text{B4})$$

one can establish that

$$\lim_{\beta \rightarrow \infty} \frac{\theta_3 \left( \pi(x + \frac{ib}{\beta\omega_0\lambda}), e^{-\frac{\pi^2}{2\beta\omega_0\lambda}} \right)}{\theta_3 \left( \pi x, e^{-\frac{\pi^2}{2\beta\omega_0\lambda}} \right)} = e^{4ibf(x)}, \quad (\text{B5})$$

where  $f(x)$  is a saw-tooth function introduced in (59), as well as that

$$\lim_{\beta \rightarrow \infty} \frac{\theta_3 \left( \pi(x + \frac{m_1}{4}), e^{-\frac{\pi^2}{2\beta\omega_0\lambda}} \right)}{\theta_3 \left( \pi(x + \frac{m_2}{4}), e^{-\frac{\pi^2}{2\beta\omega_0\lambda}} \right)} \approx e^{2\beta\omega_0\lambda g_{m_1 m_2}(x)}, \quad (\text{B6})$$

where  $m_1, m_2 = 0, 1, 2, 3$  and

$$\begin{aligned} g_{m_1 m_2}(x) &= \sum_{n=1}^{\infty} \frac{(-1)^n}{\pi^2 n^2} \\ &\times [\cos \frac{\pi n}{2}(4x + m_2) - \cos \frac{\pi n}{2}(4x + m_1)]. \end{aligned} \quad (\text{B7})$$

In the Fourier series (B7) one can recognize the functions

$$\begin{aligned} g_1(x) &\equiv g_{10}(x) = -g_{01}(x) & (B8) \\ &= \left| \left\{ \frac{1}{2} + x \right\} - \frac{3}{4} \right| + \frac{1}{2} \left\{ \frac{1}{2} + x \right\} - \frac{9}{16}, \end{aligned}$$

$$\begin{aligned} g_2(x) &\equiv g_{20}(x) = -g_{02}(x) & (B9) \\ &= -\left| \{x\} - \frac{1}{2} \right| + \frac{1}{4}, \end{aligned}$$

$$\begin{aligned} g_3(x) &\equiv g_{30}(x) = -g_{03}(x) & (B10) \\ &= \left| \left\{ \frac{1}{2} - x \right\} - \frac{3}{4} \right| + \frac{1}{2} \left\{ \frac{1}{2} - x \right\} - \frac{9}{16}, \end{aligned}$$

where  $\{x\} \equiv (x \bmod 1)$  is a fractional part of  $x$ . The function  $\{x\}$  has a period 1 and possesses a property  $\{-x\} = 1 - \{x\}$ . One can notice that  $g_3(x) = g_1(-x)$ .

The other functions  $g_{m_1 m_2}$  are also expressed in terms of  $g_1, g_2, g_3$ :

$$g_{12}(x) = -g_{21}(x) = g_3(x - 1/2), \quad (B11)$$

$$g_{32}(x) = -g_{23}(x) = g_1(x + 1/2), \quad (B12)$$

$$g_{31}(x) = -g_{13}(x) = g_2(x + 1/4). \quad (B13)$$

We also define the following functions

$$\begin{aligned} B_2 &= \tilde{\nu}_c g_2(k_\mu) + \lambda_c g_2(k_\Phi) + \nu_s g_2(k_B) + \lambda_s g_2(k_R), \\ B_3 &= \tilde{\nu}_c g_2(k_\mu) + \lambda_c g_2(k_\Phi), \\ B_4 &= \nu_s g_2(k_B) + \lambda_s g_2(k_R), \\ B_5 &= \tilde{\nu}_c g_2(k_\mu) + \nu_s g_2(k_B), \\ B_6 &= \tilde{\nu}_c g_2(k_\mu) + \lambda_s g_2(k_R), \\ B_7 &= \lambda_c g_2(k_\Phi) + \nu_s g_2(k_B), \\ B_8 &= \lambda_c g_2(k_\Phi) + \lambda_s g_2(k_R), \\ B_9 &= \tilde{\nu}_c g_1(k_\mu) + \lambda_c g_1(k_\Phi) + \nu_s g_1(k_B) + \lambda_s g_1(k_R), \\ B_{10} &= \tilde{\nu}_c g_3(k_\mu) + \lambda_c g_3(k_\Phi) + \nu_s g_3(k_B) + \lambda_s g_3(k_R), \\ B_{11} &= \tilde{\nu}_c g_3(k_\mu) + \lambda_c g_3(k_\Phi) + \nu_s g_1(k_B) + \lambda_s g_1(k_R), \\ B_{12} &= \tilde{\nu}_c g_1(k_\mu) + \lambda_c g_1(k_\Phi) + \nu_s g_3(k_B) + \lambda_s g_3(k_R), \\ B_{13} &= \tilde{\nu}_c g_3(k_\mu) + \lambda_c g_1(k_\Phi) + \nu_s g_3(k_B) + \lambda_s g_1(k_R), \\ B_{14} &= \tilde{\nu}_c g_3(k_\mu) + \lambda_c g_1(k_\Phi) + \nu_s g_1(k_B) + \lambda_s g_3(k_R), \\ B_{15} &= \tilde{\nu}_c g_1(k_\mu) + \lambda_c g_3(k_\Phi) + \nu_s g_3(k_B) + \lambda_s g_1(k_R), \\ B_{16} &= \tilde{\nu}_c g_1(k_\mu) + \lambda_c g_3(k_\Phi) + \nu_s g_1(k_B) + \lambda_s g_3(k_R). \end{aligned}$$

<sup>1</sup> Y. Aharonov and D. Bohm, Phys. Rev. **115**, 485 (1959).  
<sup>2</sup> Y. Aharonov and A. Casher, Phys. Rev. Lett. **53**, 319 (1984).  
<sup>3</sup> M. König *et al.*, cond-mat/0508396.  
<sup>4</sup> A. F. Morpurgo, J. P. Heida, T. M. Klapwijk, B. J. van Wees, and G. Borghs, Phys. Rev. Lett. **80**, 1050 (1998). See also H. De Raedt, Phys. Rev. Lett. **83**, 1700 (1999); A. F. Morpurgo, J. P. Heida, T. M. Klapwijk, B. J. van Wees, and G. Borghs, Phys. Rev. Lett. **83**, 1701 (1999).  
<sup>5</sup> T. Bergsten, T. Kobayashi, Y. Sekine, and J. Nitta, cond-mat/0512264.  
<sup>6</sup> T. Koga, Y. Sekine, and J. Nitta, cond-mat/0504743.  
<sup>7</sup> J. Nitta, T. Akazaki, H. Takayanagi, and T. Enoki, Phys. Rev. Lett. **78**, 1335 (1997).  
<sup>8</sup> Yu. A. Bychkov and E. I. Rashba, J. Phys. C **17**, 6039 (1984).  
<sup>9</sup> S. Datta and B. Das, Appl. Phys. Lett. **56**, 665 (1990).  
<sup>10</sup> M. Büttiker, Y. Imry, and M. Ya. Azbel, Phys. Rev. A **30**, 1982 (1984); M. Büttiker, Y. Imry, R. Landauer, and S. Pinhas, Phys. Rev. B **31**, 6207 (1985).  
<sup>11</sup> A. Stern, Phys. Rev. Lett. **68**, 1022 (1992).  
<sup>12</sup> A. G. Aronov and Y. B. Lyanda-Geller, Phys. Rev. Lett. **70**, 343 (1993).  
<sup>13</sup> J. Nitta, F.E. Meijer, and H. Takayanagi, Appl. Phys. Lett. **75**, 695 (1999).

<sup>14</sup> D. Frustaglia and K. Richter, Phys. Rev. B **69**, 235310 (2004).  
<sup>15</sup> B. Molnár, F. M. Peeters, and P. Vasilopoulos, Phys. Rev. B **69**, 155335 (2004).  
<sup>16</sup> J. M. Kinaret, M. Jonson, R. I. Shekhter, and S. Eggert, Phys. Rev. B **57**, 3777 (1998).  
<sup>17</sup> D. Boese, M. Governale, A. Rosch, and U. Zülicke, Phys. Rev. B **64**, 085315 (2001).  
<sup>18</sup> O. M. Auslaender, A. Yacobi, R. de Picciotto, K. W. Baldwin, L. N. Pfeiffer, and K. W. West, Science **295**, 825 (2002).  
<sup>19</sup> A. Furusaki and N. Nagaosa, Phys. Rev. B **47**, 3827 (1993).  
<sup>20</sup> J. von Delft and H. Schoeller, Annalen Phys. **7**, 225 (1998).  
<sup>21</sup> R. Fazio, F. W. J. Hekking, and A. A. Odintsov, Phys. Rev. Lett. **74**, 1843 (1995); Phys. Rev. B **53**, 6653 (1996).  
<sup>22</sup> D. Loss, Phys. Rev. Lett. **69**, 343 (1992).  
<sup>23</sup> M. R. Geller and D. Loss, Phys. Rev. B **56**, 9692 (1997).  
<sup>24</sup> M. V. Moskalets, Physica B **291**, 350 (2000).  
<sup>25</sup> M. Pletyukhov and V. Gritsev, Phys. Rev. B **70**, 165316 (2004).  
<sup>26</sup> I. V. Krive, A. M. Kadigrobov, R. I. Shekhter, and M. Jonson, Phys. Rev. B **71**, 214516 (2005).  
<sup>27</sup> G. D. Mahan, *Many-Particle Physics* (Plenum Press, NY, 1990).